RSC Advances

PAPER

View Article Online
View Journal | View Issue

Cite this: *RSC Adv.*, 2022, **12**, 1904

Synergistic advanced oxidation process for enhanced degradation of organic pollutants in spent sulfuric acid over recoverable apricot shell-derived biochar catalyst†

Jinling Zhang, Xin Jin, Hui Zhao* and Chaohe Yang*

The sulfuric acid-based alkylation process, which leads the industrial application market, still struggles with effectively removing a large number of organic pollutants from hazardous spent sulfuric acid. A synergistic advanced oxidation process was constructed to degrade the organic pollutants with H_2O_2 and sodium persulfate as the synergistic oxidants and apricot shell-derived biochar (OBC) as the catalyst. Taking the total organic carbon (TOC) and the color scale as the indices, the effects of critical experimental factors, *i.e.*, reaction temperature, initial oxidant concentration, catalyst dosage, and aeration rate, were optimized. The results showed that the removal rates of TOC and the color of the spent sulfuric acid reached ~91% and 96.6%, respectively, after 150 min under the optimum conditions. Besides, the efficient and low-cost OBC catalyst developed in this study could be continuously used for at least four times with about 75% TOC removal and 80% color removal, exhibiting favorable stability and good resistance to acid corrosion. Further study confirmed that the $SO_4^{-\bullet}$ and $^{\bullet}OH$ radicals generated in the synergistic advanced oxidation process strengthened the degradation and elimination of organic pollutants. The synergistic advanced oxidation process could provide a feasible insight for spent sulfuric acid treatment.

Received 22nd October 2021
Accepted 27th December 2021

DOI: 10.1039/d1ra07814c

rsc.li/rsc-advances

1. Introduction

Alkylated oil is an ideal blending component of reformulated gasoline with high-octane number, high antiknock index, wide boiling point range, and low content of aromatics and alkenes.[1] In 2020, the production of alkylated oil in China was more than 10×10^6 t, and over 60% alkylated oil was produced from the sulfuric acid-based alkylation process, which consequently discharged almost 10^6 t spent sulfuric acid from alkylation. Spent sulfuric acid is a hazardous chemical waste with complex organic pollutants, unstable properties, and high difficulty in treatment, causing extreme waste of resources and deterioration of the ecological environment.[2,3] Some approaches have been developed to recycle the spent sulfuric acid resources, such as thermochemical pyrolysis, neutralization, diffusion dialysis, and extraction.[4–6] Among the above methods, thermochemical pyrolysis is most widely employed to treat spent sulfuric acid at 1000–1100 °C, and the organic pollutants in spent sulfuric acid could be removed thoroughly. However, thermochemical pyrolysis is limited by the significant disadvantages of energy-extensive consumption, high investment cost, and severe equipment corrosion. It is essential to develop cost-effective and environment-friendly techniques to effectively dispose of spent sulfuric acid and obtain additional value chemical products like sulfates.[7,8]

Advanced oxidation processes (AOPs) have been alternative to degrade refractory organic pollutants into small molecules, CO_2 and H_2O, with oxidants (H_2O_2, persulfates, and O_3, etc.) by generating highly reactive radicals.[9,10] AOPs have the characteristics of being economical, eco-friendly, value-added, and low installation complexity, which could be applied to the treatment of spent sulfuric acid.[11] Fenton reaction is one of the general AOPs to effectively and rapidly degrade organic pollutants in the aqueous solutions, and the iron salts could catalyze H_2O_2 to generate highly powerful $^{\bullet}OH$ radical with the redox potential of 2.8 V.[12–14] However, the practical application of the Fenton reaction is limited due to the narrow pH range and separation difficulty of iron sludge.[15,16]

Research on using activated carbon as a green catalyst for AOPs has recently aroused extensive attention. Activated carbon could avoid introducing additional metal impurities, be resistant to strong acids or alkalis, and easily separate from the reaction solutions.[17–19] However, the practical application of commercial activated carbon is constricted because of its expensive cost, low stability, and low degradation efficiency.[20,21] The main reason for this phenomenon is the reduction of specific surface area and the decrease in active sites of activated

State Key Laboratory of Heavy Oil Processing, China University of Petroleum, Qingdao, Shandong 266580, People's Republic of China. E-mail: zhaohui@upc.edu.cn; yangch@upc.edu.cn

† Electronic supplementary information (ESI) available. See DOI: 10.1039/d1ra07814c

carbon catalyst.[22] Biochar is considered as an alternative catalyst with favorable physicochemical properties, which could be prepared from agricultural residues such as cornstalk, sugarcane bagasse, coconut shell, and apricot shell.[23–25] Especially, biochar with various functions such as waste disposal and wastewater remediation could be obtained through different physical or chemical activation procedures.[26,27] However, the previous studies on biochar mainly concentrated on its adsorption of organic pollutants in wastewater or soil. In contrast, the adsorption capacity of biochar decreases with the saturation of adsorption sites.[28,29] It is promising to develop an economic and green biochar catalyst for the oxidative degradation of refractory organic pollutants in spent sulfuric acid.

This work developed and optimized a synergistic advanced oxidation process to degrade the organic pollutants in spent sulfuric acid using H_2O_2 and sodium persulfate (PS) as oxidants over the apricot shell-derived biochar (OBC) catalyst. The degradation efficiency of organic pollutants was evaluated under different reaction conditions in terms of the total organic carbon (TOC) and color scale as the indexes. Besides, the stability of the OBC catalyst in the process was assessed under the optimal conditions. Furthermore, a plausible radical mechanism in the process was proposed. Finally, the changes of the organic pollutants during the process were evaluated under the optimal conditions, and the characteristics of the obtained product were also assessed. The constructed process is expected to offer a candidate strategy for spent sulfuric acid treatment.

2. Materials and methods

2.1. Materials and chemicals

The black-red and sticky spent sulfuric acid was gathered from the industrial alkylation unit (Shandong, China), which was sealed and stored under −15 °C before use. The compositions of spent sulfuric acid were determined by the titration method, which was 91.34 wt% sulfuric acid, 3.48 wt% water, and 5.18 wt% acid-soluble oil. The characteristics of spent sulfuric acid were listed in Table 1. The spent sulfuric acid was used as soon as possible because its property changes with time.

Hydrogen peroxide (30 wt% H_2O_2), ethanol (EtOH, CH_3-CH_2OH), and *tert*-butyl alcohol (TBA, C_4H_9OH) were obtained from Sinopharm Chemical Reagent Co., Ltd (Shanghai, China). Sodium persulfate (PS, $Na_2S_2O_8$) and 5,5-dimethyl-1-pyrolin-*N*-oxide (DMPO) were supported by Sigma-Aldrich (China). The feedstock for the preparation of OBC in this study was an apricot shell residue, which was collected from Haizhou Water Treatment Materials Co., Ltd (Henan, China). All the solutions were prepared in deionized water.

Table 1 Initial characteristics of spent sulfuric acid gathered from Shandong, China[a]

Parameter	Unit	Value
COD	mg L^{-1}	238 000
TOC	mg L^{-1}	57 500
Density (20 °C)	g cm^{-3}	1.676
Viscosity (25 °C)	mPa s	17.15
Suspended solids	wt%	1.59
Color	Times	80 000
C (H^+)	mol L^{-1}	32.56

[a] Noted: COD: chemical oxygen demand.

2.2. Preparation of OBC

The OBC was prepared through the carbonization and activation processes of apricot shell residues. In brief, 40 g of apricot shell residue was washed with deionized water and dried at 110 °C for 24 h. The dried sample was shattered with a planetary ball mill and sieved into 2–5 mm granular, and then put into a tubular furnace under a N_2 flow of 20 L min^{-1}. The temperature of the tubular furnace was procedurally increased from room temperature to 850 °C at about 10 °C min^{-1} and kept for 3 h. After the carbonization, the N_2 flow was switched into a collaborative atmosphere of CO_2 and N_2, and the flow rate of CO_2 was 20 L min^{-1}. The temperature of the tubular furnace was held at 850 °C for 2 h, and then cooled down to 20 °C under N_2 atmosphere. The activated sample was impregnated in 1 mol L^{-1} HCl solution for 24 h to remove the inorganic components, washed with deionized water, and then oven-dried at 110 °C before use. The resultant sample was termed OBC.

2.3. Experimental procedures

The spent sulfuric acid treatment *via* synergistic advanced oxidation process was evaluated under different conditions, including reaction temperature (50–110 °C), initial oxidants concentration (5–9 mol (L spent acid)$^{-1}$), catalyst dosage (0–1.5 wt% (spent acid weight)), and aeration rate (0–12 L min^{-1}). The experiments were conducted in a flask with a magnetic stir bar and a condenser pipe. In one typical experiment, 100 g of spent sulfuric acid was added into the flask and heated in an oil bath under a constant stirring speed of 120 rpm. After the solution was heated to the desired temperature of 100 °C, 1.0 g of OBC granular was added, and continuous air was simultaneously injected into the solution using an air pump at a constant flow rate of 10 L min^{-1}. Meanwhile, 0.26 mol H_2O_2 and 0.18 mol PS were dropwise dropped into the solution separately. After the required reaction time, the solution was filtered and cooled down to ambient temperature. 2 ml of the sample was collected and filtered with 0.22 μm membrane for chemical analysis at given time intervals. To evaluate the stability of the OBC catalyst, the used OBC granular was separated and recycled under the same operating conditions.

2.4. Analytical and characterization methods

The COD content of the reaction solution was measured according to the standard methods of HJ/T 399-2007 in China,[23] the TOC content was measured by a TOC-V_{CPN} analyzer (Shimadzu), and the color scale of the reaction solution was determined by the dilution multiple methods. The contents of C, H, S, N elements in spent sulfuric acid and treated sulfuric acid were obtained with a Vario EL III Elementary, and the samples were absorbed by SiO_2 before elemental analysis since they were corrosive. The compositions of the organic pollutants in spent

sulfuric acid and treated sulfuric acid were analyzed by a gas chromatography-mass spectrometry (GC-MS 7890A-5975C, Agilent) with a HP-5MS column (30 m × 0.25 mm × 0.25 μm). The organic pollutants were extracted from spent sulfuric acid in sequence using trichloromethane under neutral, alkaline, and acidic conditions, and the organic phase was concentrated to 1.0 ml with a rotary evaporator (ZFQ85A). High purity helium was used as carrier gas at a rate of 1.0 ml min^{-1} in GC-MS analysis. The detector temperature was 270 °C, and the column was initially set at 50 °C for 3 min, heated to 270 °C at 8 °C min^{-1} and maintained for 10 min. Mass spectrometry analysis of the compounds was tested in a m/z range of 25–400. The injector temperature was 50 °C, and the ionization energy was 70 eV. The National Institute of Standards and Technology (NIST) spectral database was used to identify the main compositions of organic pollutants.

Free radicals trapped by DMPO in the reaction solution were observed by an electron paramagnetic resonance spectrometer (ESR, Bruke Emx plus, Germany). X-ray fluorescence (XRF), surface chemistry, porous structures, scanning electron microscopy (SEM), Fourier transform infrared spectroscopy (FT-IR), and X-ray photoelectron spectroscopy (XPS) of OBC were characterized. More detailed analytical and characterization conditions could be found in the ESI.†

3. Results and discussion

3.1. Degradation performance comparison for different systems

Spent sulfuric acid treatment was carried out in the oxidants system, oxidants/OBC system, oxidants/aeration system, and synergistic advanced oxidation process, respectively. Compared with the other reaction systems, the synergistic advanced oxidation process showed apparently higher TOC and color removals (Fig. 1a and b). Besides, all of the reaction systems were fitted by the pseudo-first-order kinetic model (Fig. 1c), and the rate constant of TOC (0.0161 min^{-1}) in the synergistic advanced oxidation process was greater than the other reaction systems, suggesting that there existed an apparent synergistic effect between the oxidants, catalyst, and aeration. Similar results related to the synthetic systems were also reported by other researchers.[30] According to the results of the synergistic advanced oxidation process, the TOC removal increased rapidly from 0 to 150 min (Fig. 1a), and the color of the reaction solution changed obviously from black-brown to almost colorless (Fig. 1d), indicating that most of the chromophore substances in spent sulfuric acid were virtually removed. As the reaction time excessed 150 min, the TOC removal increased slightly and tended to be stable. The color of the solution was pale yellow shades, which may be because some hydrophilic or low-

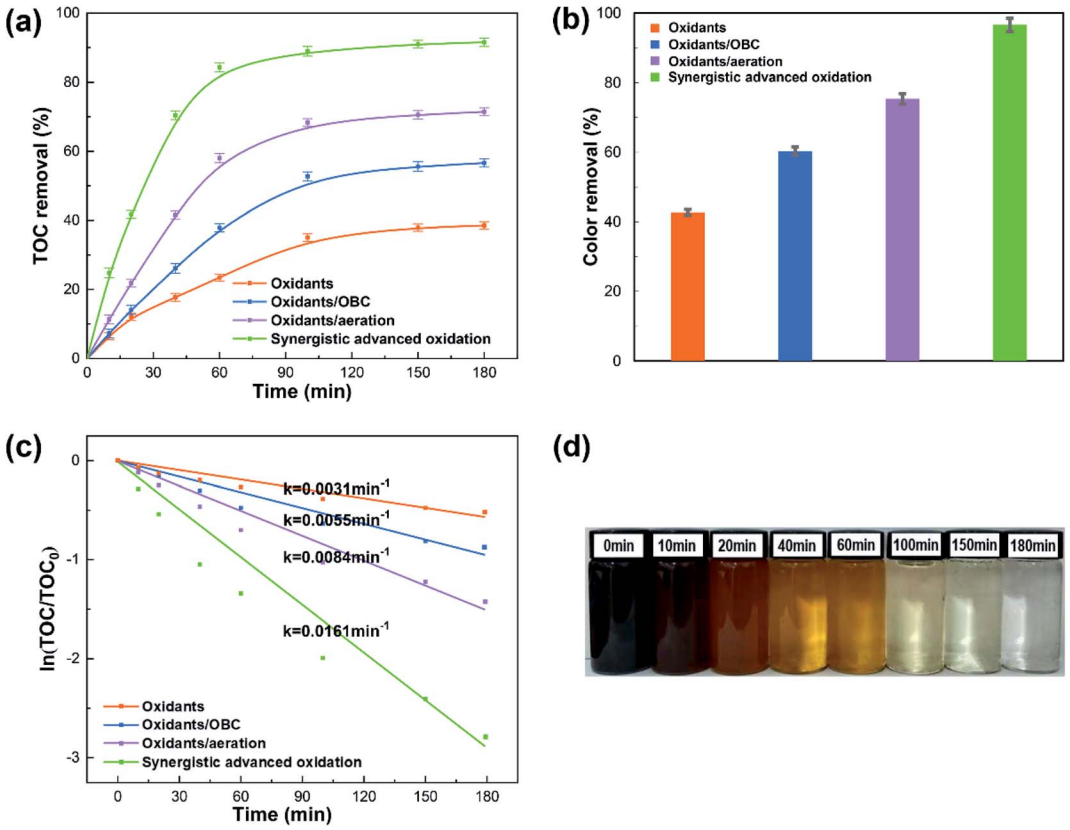

Fig. 1 (a) Removal rate of TOC under different reaction systems, (b) removal rate of color under different reaction systems, (c) pseudo-first-order kinetic plot of TOC under different reaction systems, and (d) color change of the sulfuric acid solution with different reaction time in the synergistic advanced oxidation process (initial oxidants concentration = 8 mol (L spent acid)$^{-1}$, catalyst dosage = 1.0 wt% (spent acid weight), aeration rate = 10 L min^{-1}, reaction temperature = 100 °C).

molecule matters remained in the sulfuric acid solution. It was found that the TOC and color removals in the synergistic advanced oxidation process reached 90.99% and 96.57%, respectively, under the optimal reaction time of 150 min, demonstrating that the effective removal of organic pollutants was achieved.

3.2. Effects of operational factors

In this part, the effects of reaction temperature, initial oxidants concentration, catalyst dosage, and aeration rate on the degradation of organic pollutants in the synergistic advanced oxidation process were investigated through the single-factor experiments.

3.2.1. Effect of reaction temperature. It is well known that the reaction temperature has a significant impact on the oxidation ability of AOPs. The effect of reaction temperature varying from 50 °C to 110 °C on the degradation performance of organic pollutants was estimated in this study (Fig. 2a). The TOC and color removals were relatively slow as the reaction temperature was below 70 °C, but they accelerated as the reaction temperature exceeded 80 °C, indicating that a high reaction temperature could promote the removal of organic pollutants. The reasonable explanation was that the increase in temperature accelerated the generation of active species and decreased the viscosity of the reaction solution to promote the mass transfer process, which was suitable for the reaction rate of organic pollutants in spent sulfuric acid. However, the TOC and color removals slightly increased as the temperature was higher than 100 °C, ascribing to that the decomposition of H_2O_2 and PS at excessive temperature could reduce the generation of active species for the removal of organic pollutants, and the foaming and fog entrainment formed in the reaction solution could cause the operational hazards. Therefore, based on cost-saving and efficiency, the reaction temperature of around 100 °C was adapted in the following experiments.

3.2.2. Effect of initial oxidants concentration. The effect of initial oxidants concentration on the oxidative degradation of organic pollutants was assessed in this work, and the molar ratio of H_2O_2 to PS was kept at 3 : 2 (Fig. 2b). For the proposed process with the initial oxidants' concentration from 5 to 8 mol (L spent acid)$^{-1}$, the TOC removal increased from 56.78% to 90.99% after 150 min, and the color removal increased from 62.43% to 96.57% within the same time. The rising initial oxidants concentration effectively enhanced the degradation efficiency of organic pollutants, which was closely related to that the production of free radicals, such as $SO_4-^{\bullet}$, $^{\bullet}OH$ and $^{\bullet}HO_2$, increased with the increasing initial oxidants concentration. However, both the TOC and color removals reduced slightly when the concentration of the initial oxidant exceeded 8 mol (L spent acid)$^{-1}$, which was due to the scavenging effect of free radicals and the self-decomposition reaction of H_2O_2 and PS.[31] Consequently, the concentration of the initial oxidant of 8 mol (L spent acid)$^{-1}$ was considered as the optimal condition in the process, which was much less than that for a typical oxidation reaction to achieve the same removal of organic pollutants.[26]

3.2.3. Effect of catalyst dosage. In this experiment, the removal efficiency of organic pollutants was evaluated under different dosages of OBC catalyst from 0 to 1.5 wt% (Fig. 2c). As the catalyst dosage increased from 0 to 1.0 wt%, the removal rates of TOC and color enhanced obviously both in the OBC adsorption system and the synergistic advanced oxidation process. This was due to the increased dosage of OBC with sufficient acidic oxygen surface groups and anchored metal ions could provide more active sites (Table 2), which strengthened the activation of OBC to oxidants to generate higher concentration of free radicals, thereby significantly increased the degradation efficiency of organic pollutants.[29,32] Additionally, OBC with a rough surface and porous structure was prepared from the carbonization and activation of biomacromolecules, which offered ample surface area for adsorption and the activation of oxidants to produce radicals. However, the TOC and color removals slightly increased as the catalyst dosage exceeded 1.0 wt% in the synergistic advanced oxidation process. The reason may be that the absorbed and saturated organic pollutants on OBC surface reduced the active sites accessible for the activation of oxidants, which had an adverse effect on the degradation of organic pollutants.[33]

Based on the above results, the optimal catalyst dosage in the synergistic advanced oxidation process was 1.0 wt% (spent acid weight), which was less than those for oxidation reaction with carbon materials as catalysts for spent sulfuric acid treatment.[26,28] Compared with the preparation process of traditional activated carbon, a low-cost and straightforward manufacturing route to obtain biochar catalysts from agricultural residues was developed in this study, which could effectively reduce the treatment cost of spent sulfuric acid.

3.2.4. Effect of aeration rate. To investigate the effect of aeration rate on the degradation performance of organic pollutants, several experiments were conducted with the aeration rate from 0 to 12 L min^{-1} and the results were illustrated in Fig. 2d. The results indicated that the removal rates of TOC and color after 150 min were 55.56% and 59.46% without aeration. As the aeration rate increased from 2 to 10 L min^{-1}, the TOC removal increased from 72.18% to 90.99%, and the color removal rose from 77.77% to 96.57%. The phenomenon may be that the amounts of free radicals such as $^{\bullet}OH$, $^{\bullet}HO_2$ and $^{\bullet}O_2-$ increased as the aeration rate increased, promoting the deep oxidative degradation of organic pollutants during the synergistic advanced oxidation process.[34] In addition, it was reported that the increased aeration rate had a strong agitation effect on the reaction system, and the mass transfer effect was accordingly enhanced.[35] The TOC and color removals increased slowly when the aeration rate exceeded 10 L min^{-1}, which meant that the oxidative degradation reaction of organic pollutants reached equilibrium at some critical aeration rate. Therefore, the aeration rate in the process was optimized to be 10 L min^{-1}.

3.3. Stability of OBC catalyst

To evaluate the potential reusability of the OBC catalyst, OBC was sequentially used in the synergistic advanced oxidation process (Fig. 3). Fig. 3 indicated that the removals of TOC and

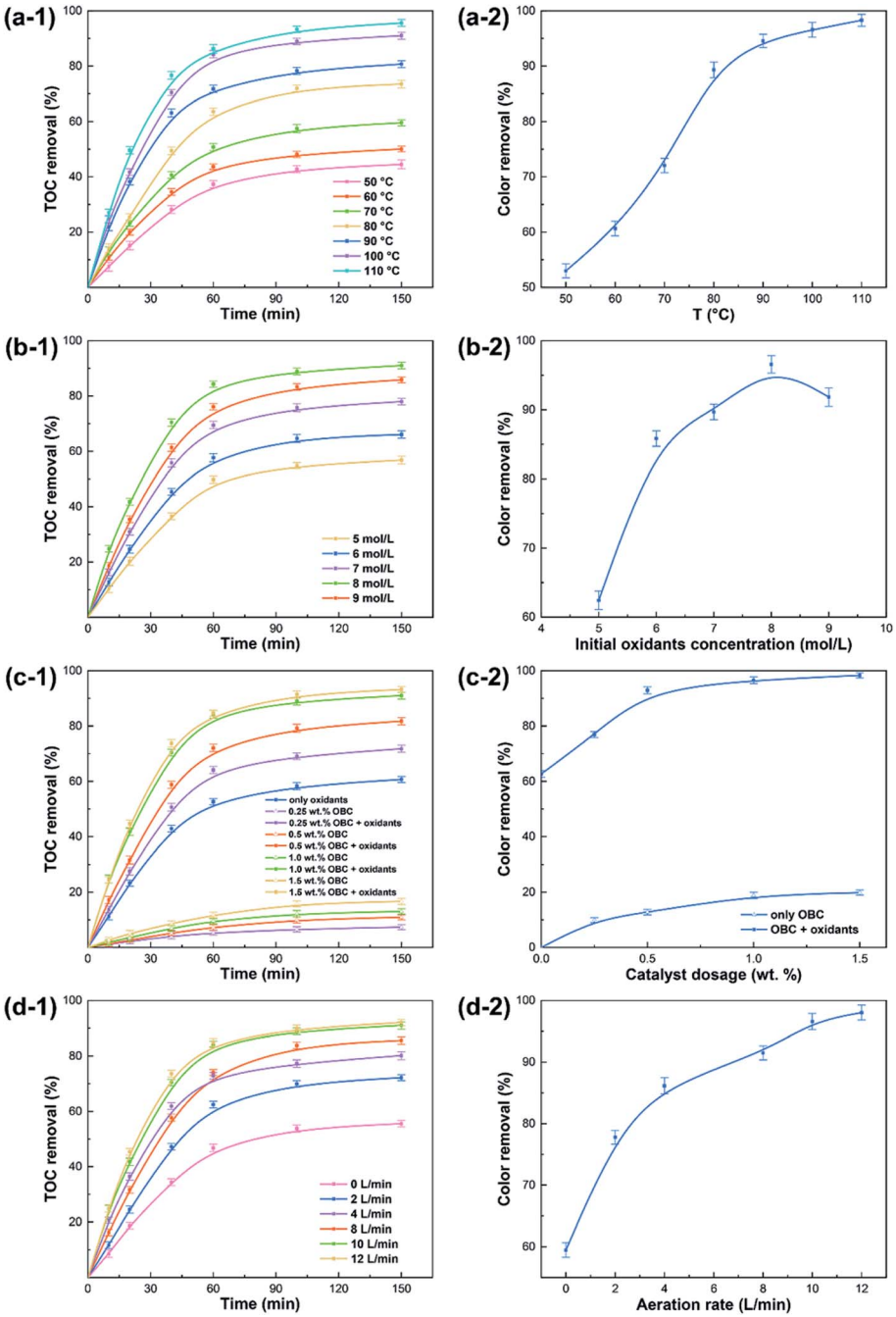

Fig. 2 Effect of reaction temperature on the (a-1) TOC removal and (a-2) color removal in the synergistic advanced oxidation process (initial oxidants concentration = 8 mol (L spent acid)$^{-1}$, catalyst dosage = 1.0 wt% (spent acid weight), aeration rate = 10 L min^{-1}, reaction time = 150 min), effect of initial oxidants concentration on the (b-1) TOC removal and (b-2) color removal in the synergistic advanced oxidation process (catalyst dosage = 1.0 wt% (spent acid weight), aeration rate = 10 L min^{-1}, reaction temperature = 100 °C, reaction time = 150 min), effect of catalyst dosage on the (c-1) TOC removal and (c-2) color removal in the synergistic advanced oxidation process (initial oxidants concentration = 8 mol (L spent acid)$^{-1}$, aeration rate = 10 L min^{-1}, reaction temperature = 100 °C, reaction time = 150 min), and effect of aeration rate on the (d-1) TOC removal and (d-2) color removal in the synergistic advanced oxidation process (initial oxidants concentration = 8 mol (L spent acid)$^{-1}$, catalyst dosage = 1.0 wt% (spent acid weight), reaction temperature = 100 °C, reaction time = 150 min).

color unavoidably declined as the OBC cycles increased, maybe attributing to the mass loss (about 10 wt% per cycle) caused by filtration and cleaning during the recovery of OBC. The TOC and color removals after 150 min remained 74.72% and 79.65% in the fourth reaction cycle, indicating that OBC exhibited good acid resistance in the spent sulfuric acid treatment. However, the TOC and color removals decreased remarkably in the fifth reaction cycle, implying that the process's ability to remove organic pollutants decreased rapidly. This phenomenon could be attributed to the sharp loss of acidic oxygen surface groups

Table 2 Characteristics of OBC

Characteristics	Values
Yield (%)	37.2
Ash (%)	5.18
pH_{PZC}	2.23
Total acidity (mmol g^{-1})	2.012
O (%)	27.78
Na (%)	0.083
Mg (%)	0.083
Al (%)	0.22
P (%)	1.575
S (%)	7.866
K (%)	22.52
Ca (%)	17.54
Fe (%)	1.41
Cu (%)	0.182

on the surface of OBC reduced the amounts of active sites (Table 3), and hence reduced the production of radicals to degrade the organic pollutants.[36] In addition, partial active sites on OBC were likely taken up by the absorbed organic contaminants and intermediate products, reducing their ability to activate the oxidants to generate sufficient free radicals.[37] It was found that both the specific surface area (784 m^2 g^{-1}) and the total pore volume (0.413 cm^3 g^{-1}) of OBC after four continuous reactions were lower than those before the reaction (Table 4), which confirmed the blockage of the porous structure of OBC.

SEM images of OBC and OBC after four continuous reactions were shown in Fig. 4. The morphology of OBC showed large macropores at the micrometer scale with irregular shape and rough surfaces (Fig. 4a), indicating that the biomacromolecules carbonized to form porous structures during the pyrolysis. Nevertheless, progressive surface changes could be observed after four continuous reactions in Fig. 4b. The carbon surface became more bulging and rougher, which was likely attributed to the strong effect of the oxidants and sulfuric acid during the reaction.

The surface chemical properties of OBC and OBC after four continuous reactions were analyzed by FT-IR and XPS techniques. As shown in the FTIR spectra (Fig. 5), the peaks of OBC in the range of 3700–3200, 1680–1560, and 1150–1050 cm^{-1} were assigned to the stretching of O–H, C=O, and C–O, respectively.[14] The above characteristic peaks in OBC decreased obviously after four continuous reactions, which was related to the loss of phenol, carboxyl and lactone groups on the surface of OBC. Moreover, the XPS O 1s spectra of OBC and OBC after four continuous reactions were compared, and the O 1s peaks at 531.9–531.7 eV and 533.0 eV corresponded to the C=O and C–O, respectively (Fig. 6). It was found that the peaks of the C=O and

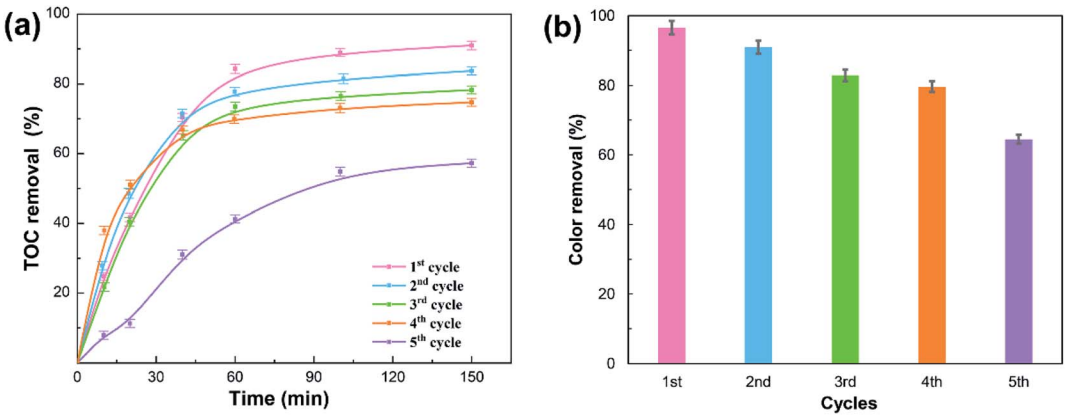

Fig. 3 The stability of OBC in the synergistic advanced oxidation process (initial oxidants concentration = 8 mol (L spent acid)$^{-1}$, catalyst dosage = 1.0 wt% (spent acid weight), aeration rate = 10 L min^{-1}, reaction temperature = 100 °C, reaction time = 150 min).

Table 3 The number of acidic oxygen surface groups of OBC before and after 4 continuous reactions

Sample	Carboxyl (mmol g^{-1})	Lactone (mmol g^{-1})	Phenol (mmol g^{-1})	Carbonyl (mmol g^{-1})	Acidic (mmol g^{-1})
OBC	0.932	0.488	0.524	0.068	2.012
OBC after reaction	0.654	0. 334	0.371	0.043	1.068

Table 4 Porous structure of OBC before and after 4 continuous reactions

Sample	S_{BET} (m^2 g^{-1})	S_{mic} (m^2 g^{-1})	V_{total} (cm^3 g^{-1})	V_{mic} (cm^3 g^{-1})	D (nm)
OBC	1088	981	0.463	0.396	2.57
OBC after reaction	784	659	0.413	0.337	3.21

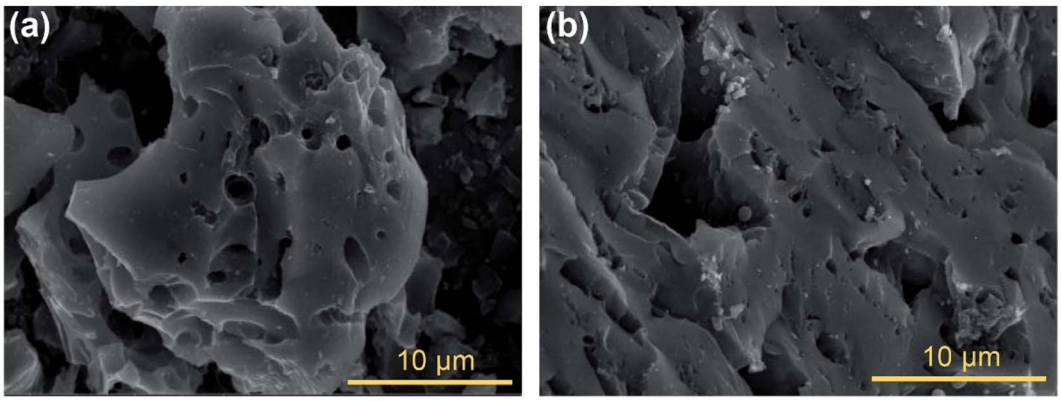

Fig. 4 SEM images of OBC (a) before and (b) after 4 continuous reactions.

C–O on the surface of OBC became weaker after four continuous reactions, which further confirmed the decrease in the acidic oxygen surface groups on OBC. The results showed that the reduction of acidic oxygen surface groups on the surface of OBC might be the main reason for the decreasing degradation rate of organic pollutants after continuous reactions.

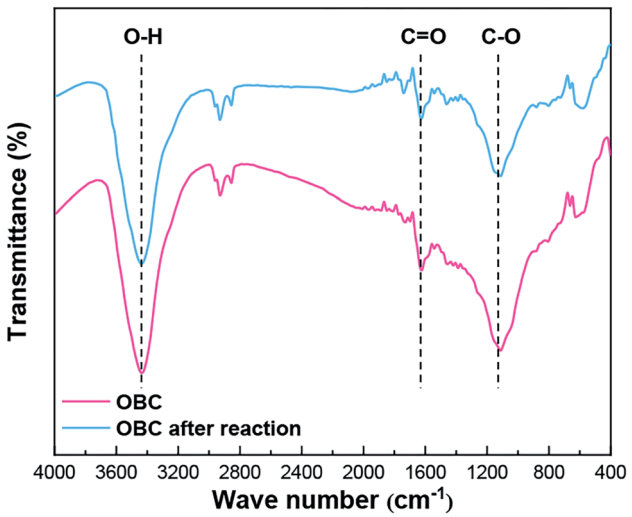

Fig. 5 FT-IR spectra of OBC before and after 4 continuous reactions.

3.4. Plausible radical mechanism

To explore the plausible radical mechanism of the synergistic advanced oxidation process, a series of trapping tests to monitor the free radicals were conducted. As shown in Fig. 7a, the TOC removal was inhibited in the presence of TBA (scavenger of ˙OH) and EtOH (scavenger of SO_4−˙ and ˙OH), conforming that SO_4−˙ and ˙OH radicals were the principle free radicals in the process.[38] In addition, the ESR spectra of free radicals under different systems were determined using DMPO as the spin trap agent (Fig. 7b). The characteristic signals attributed to ˙OH, ˙HO_2, and SO_4−˙ radicals were simultaneously observed in the synergistic advanced oxidation process.[32] The intensity of the signals in the above process was much higher than the other systems, indicating that plentiful free radicals were generated in the process. The schematic diagram of the plausible radical mechanism was shown in Fig. 7c. The above analyses demonstrated that the synergistic advanced oxidation process was favorable to the strengthened radical reactions, achieving the rapid and efficient degradation efficiency of organic pollutants (eqn (1)).

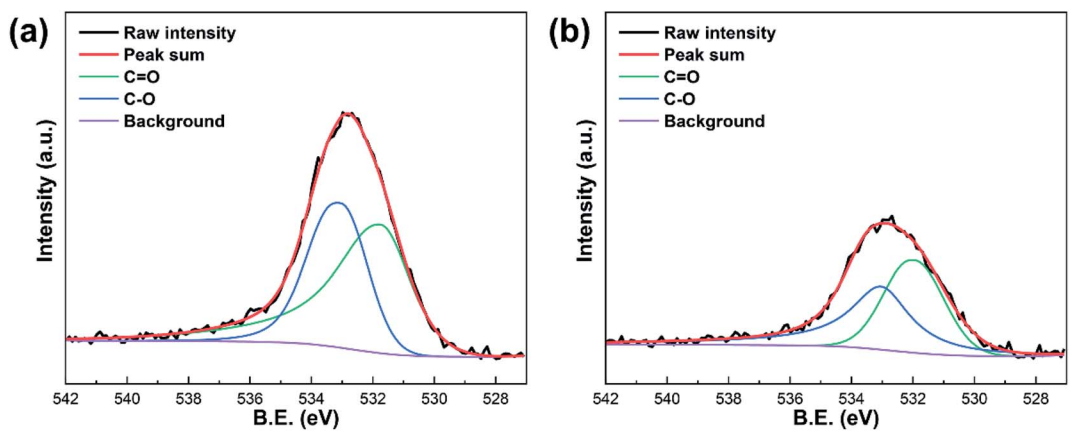

Fig. 6 XPS O 1s spectra of OBC (a) before and (b) after 4 continuous reactions.

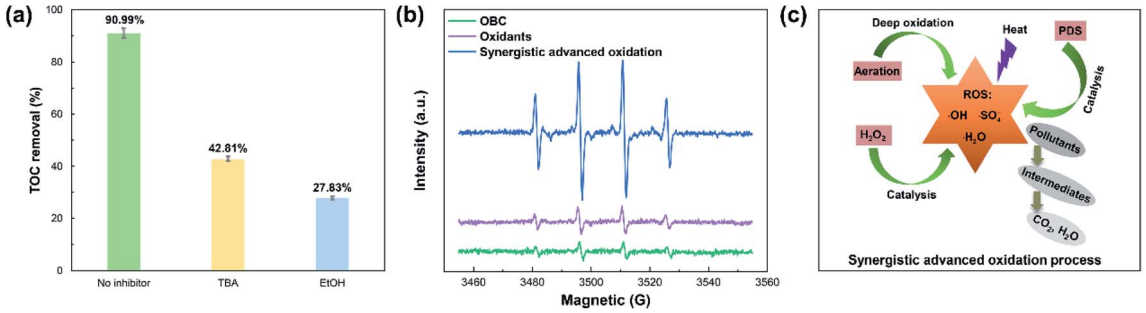

Fig. 7 (a) Effect of the free radical inhibitors on TOC removal in the synergistic advanced oxidation process, (b) DMPO trapped ESR spectra of radicals under different reaction systems, and (c) plausible radical mechanism of the synergistic advanced oxidation process.

$$\text{Organic pollutants} + \text{free radicals} \rightarrow \text{intermediates} \rightarrow CO_2 + H_2O \quad (1)$$

3.5. Analysis of the H_2SO_4 solution during the synergistic advanced oxidation process

To investigate the degradation efficiency of organic pollutants by the synergistic advanced oxidation process, the H_2SO_4 solutions before and after the reaction were detected by elemental analysis (Table 5). After 150 min, the carbon content in the H_2SO_4 solution decreased from 2.76 to 0.04 wt%, indicating that a vast majority of the organic pollutants were effectively degraded during the reaction.

Table 5 Elemental analysis of spent sulfuric acid and treated sulfuric acid (wt%). (Initial oxidants concentration = 8 mol (L spent acid)$^{-1}$, catalyst dosage = 1.0 wt% (spent acid weight), aeration rate = 10 L min^{-1}, reaction temperature = 100 °C, reaction time = 150 min)

Sample	Carbon	Hydrogen	Sulfur	Nitrogen
Spent sulfuric acid	2.76	2.52	28.74	—
Treated sulfuric acid	0.04	1.76	30.08	—

GC-MS was applied to further investigate the changes of primary organic pollutants during the reaction (Fig. 8). Compared with Fig. 8a, the number of the detected peaks in treated sulfuric acid decreased apparently with weakened intensity, indicating that the contents and types of the organic pollutants decreased significantly after the oxidation reaction, which was consistent with the result of elemental analysis. Additionally, the refractory polycyclic macromolecular organic matters such as bisphenol P ($C_{24}H_{26}O_2$), diethylene glycol dibenzoate ($C_{18}H_{18}O_5$), and oxydipropyl dibenzoate ($C_{20}H_{22}O_5$) were detected in spent sulfuric acid (Table 6). After the oxidation reaction, the degradable monocyclic organic matters like 1,1,3-trimethylcyclohexane (C_9H_{18}) and 6,6-dimethyl-2-cyclohexen-1-ol ($C_8H_{14}O$) were identified in the treated sulfuric acid (Table 6). The mass spectra of the detected organic pollutants in spent sulfuric acid and treated sulfuric acid could be found in Fig. S1–S2.† The degradation mechanism of the organic pollutants may be that the oxidants (H_2O_2 and PS) and the generated free radicals ($^{\cdot}OH$, $^{\cdot}HO_2$, and $SO_4^{-\cdot}$) could attack the macromolecules, and occur the relevant radical reactions such as hydrogen abstraction, double bond addition, electron transfer, and bond cleavage, leading to the formation of CO_2, H_2O, and small molecular compounds. Therefore, the

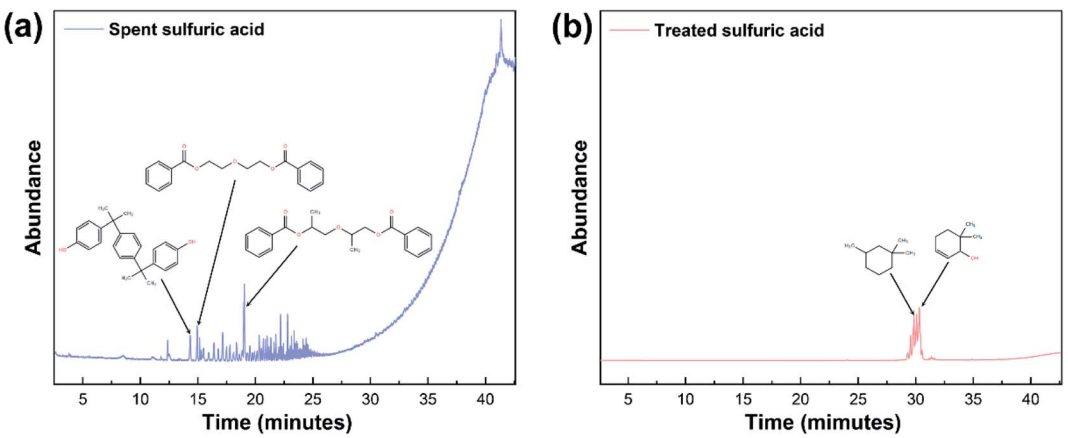

Fig. 8 GC-MS chromatogram of the organic pollutants in (a) spent sulfuric acid and (b) treated sulfuric acid after the synergistic advanced oxidation process (initial oxidants concentration = 8 mol (L spent acid)$^{-1}$, catalyst dosage = 1.0 wt% (spent acid weight), aeration rate = 10 L min^{-1}, reaction temperature = 100 °C, reaction time = 150 min).

Table 6 Main organic pollutants detected in spent sulfuric acid and treated sulfuric acid by GC-MS

Sample	Compound	Formula	R_t (min)	m/z
Spent sulfuric acid	Bisphenol P 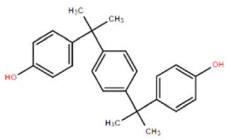	$C_{24}H_{26}O_2$	14.331	28, 32, 149, 253, 254, 255, 269, 331, 332, 346
	Diethylene glycol dibenzoate 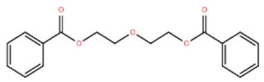	$C_{18}H_{18}O_5$	14.937	51, 70, 76, 77, 78, 105, 106, 149, 150, 163
	Oxydipropyl dibenzoate 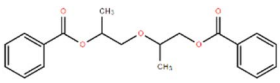	$C_{20}H_{22}O_5$	19.045	28, 43, 57, 77, 105, 106, 149, 163, 164, 207
Treated sulfuric acid	1,1,3-Trimethylcyclohexane 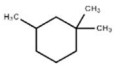	C_9H_{18}	29.854	28, 32, 41, 43, 55, 69, 83, 106, 111, 147
	6,6-Dimethyl-2-cyclohexen-1-ol 	$C_8H_{14}O$	30.324	28, 39, 41, 55, 56, 67, 70, 95, 111, 126

proposed synergistic advanced oxidation process realized the deep degradation and removal of the organic pollutants in spent sulfuric acid.

3.6. Identification of the product

The resulting treated sulfuric acid with TOC removal of 90.99% and color removal of 96.57% was acquired under the optimum reaction conditions of initial oxidants concentration of 8 mol (L spent acid)$^{-1}$, catalyst dosage of 1.0 wt% (spent acid weight), aeration rate of 10 L min^{-1}, reaction temperature of 100 °C, and reaction time of 150 min. The H_2SO_4 content was 91.34 wt% in the clear colorless product, and the recovery of H_2SO_4 was up to 95%. After the reaction, the content of COD decreased from 238 000 to 3570 mg L^{-1}, the content of TOC decreased from 57 500 to 5180 mg L^{-1}, and the color scale reduced from 80 000 to 2744 times, respectively (Table 7). The above results showed the efficient performance of the proposed process on the treatment of spent sulfuric acid, and the treated sulfuric acid could be further concentrated or utilized to prepare sodium sulfate.

Table 7 Characteristics of treated sulfuric acid after the synergistic advanced oxidation process

Parameter	Unit	Average value
COD	mg L^{-1}	3570
TOC	mg L^{-1}	5180
Density (20 °C)	g cm^{-3}	1.515
Viscosity (25 °C)	mPa s	6.86
Suspended solids	wt%	0.3
Color	Times	2744

4. Conclusions

This work primarily aims to provide a novel synergistic advanced oxidation process to address the spent sulfuric acid issues in the alkylation industry with apricot shell-derived biochar (OBC) as catalyst. Compared with the oxidants system, oxidants/OBC system, and oxidants/aeration system, the synergistic advanced oxidation process displayed better degradation performance of the organic pollutants. It was discovered that the removal rates of TOC and color reached approximately 91% and 97% after 150 min under the optimal conditions of initial oxidants concentration of 8 mol (L spent acid)$^{-1}$, catalyst dosage of 1.0 wt% (spent acid weight), aeration rate of 10 L min^{-1} and reaction temperature of 100 °C. The excellent performance of the proposed process was mainly due to the strengthened radical reactions, and the treated sulfuric acid with a carbon content of 0.04 wt% could be utilized to produce sodium sulfate. Besides, OBC catalyst demonstrated superior stability, reusability, and acid resistance in the process, and the TOC and color removals remained about 75% and 80% after four cycles of use. Overall, this work offered an energy-efficient approach to dispose spent sulfuric acid with hazards organic pollutants using agricultural residues-derived biochar as effective catalyst, which realized the purpose of obtaining resources from wastes.

Abbreviations

AOPs	Advanced oxidation processes;
COD	Chemical oxygen dioxide;
ESR	Electron paramagnetic resonance spectrometer;
EtOH	Ethanol;

FT-IR	Fourier transform infrared spectrometer;
GC-MS	Gas chromatography-mass spectrometry;
H_2O_2	Hydrogen peroxide;
H_2SO_4	Sulfuric acid;
$Na_2S_2O_8$	Sodiumpersulfate;
NIST	National Institute of Standards and Technology;
SEM	Scanning electron microscopy;
TBA	*tert*-Butyl alcohol;
TOC	Total organic carbon;
XPS	X-ray photoelectron spectroscopy;
XRF	X-ray fluorescence spectrometer

Author contributions

Jinling Zhang: conceptualization, methodology, investigation, writing – original draft. Xin Jin: supervision, validation, writing – review & editing. Hui Zhao: writing – review & editing. Chaohe Yang: supervision, funding acquisition, validation.

Conflicts of interest

The authors declare that they have no known competing financial interests or personal relationships that could have appeared to influence the work reported in this paper.

Acknowledgements

Our study was funded by the National Natural Science Foundation of China (21706290), the Fundamental Research Funds for the Central Universities (17CX02017A), the Natural Science Foundation of Shandong Province (ZR2017MB004), and the Postgraduate Innovation Engineering (YCX2021051).

References

1 Z. Zhou, X. Zhang, F. Yang and S. Zhang, *J. Cleaner Prod.*, 2019, **215**, 13–21.
2 X. Qi, L. Li, T. Tan, W. Chen and R. L. Smith, Jr, *Environ. Sci. Technol.*, 2013, **47**, 2792–2798.
3 A. S. Berenblyum, L. V. Ovsyannikova, E. A. Katsman, J. Zavilla, S. I. Hommeltoft and Y. Z. Karasev, *Appl. Catal., A*, 2002, **232**, 51–58.
4 F. L. Albright, *Ind. Eng. Chem. Res.*, 2009, **48**, 1409–1413.
5 L. Cifuentes, I. García, R. Ortiz and J. M. Casas, *Sep. Purif. Technol.*, 2006, **50**, 167–174.
6 A. Agrawal and K. K. Sahu, *J. Hazard. Mater.*, 2009, **171**, 61–75.
7 M. Kamarou, N. Korob, A. Hil, D. Moskovskikh and V. Romanovski, *J. Chem. Technol. Biotechnol.*, 2021, **96**, 2065–2071.
8 M. Kamarou, N. Korob, W. Kwapinski and V. Romanovski, *J. Ind. Eng. Chem.*, 2021, **100**, 324–332.
9 Z. Liu, K. Demeestere and S. V. Hulle, *J. Environ. Chem. Eng.*, 2021, **9**, 105599.
10 Z. Wang, L. Ai and Y. Huang, *RSC Adv.*, 2017, **749**, 30941–30948.
11 S. Yang, P. Wang, X. Yang, L. Shan, W. Zhang, X. Shao and R. Niu, *J. Hazard. Mater.*, 2010, **179**, 552–558.
12 Y. Tang, S. Zhao, Z. Peng, Z. Li, L. Chen and P. Gan, *RSC Adv.*, 2021, **11**, 20983–20991.
13 X. Mu, H. Ding, W. Pan, Q. Zhou, W. Du, K. Qiu, J. Ma and K. Zhang, *J. Environ. Chem. Eng.*, 2021, **9**, 105650.
14 J. H. Park, J. J. Wang, R. Xiao, N. Tafti, R. D. DeLaune and D. C. Seo, *Bioresour. Technol.*, 2018, **249**, 368–376.
15 C. Xiao, S. Li, F. Yi, B. Zhang, D. Chen, Y. Zhang, H. Chen and Y. Huang, *RSC Adv.*, 2020, **10**, 18704–18714.
16 A. D. Bokare and W. Choi, *J. Hazard. Mater.*, 2014, **275**, 121–135.
17 S. Tak and B. P. Vellanki, *J. Environ. Chem. Eng.*, 2020, **8**, 104434.
18 A. Rey, A. B. Hungria, C. J. Duran Valle, M. Faraldos, A. Bahamonde, J. A. Casas and J. J. Rodriguez, *Appl. Catal., B*, 2016, **181**, 249–259.
19 M. K. Manu, C. Wang, D. Li, S. Varjani, Y. Xu, N. Ladumor, M. Lui, J. Zhou and J. W. C. Wong, *Bioresour. Technol.*, 2021, **341**, 125871.
20 M. Pedrosa, J. L. Figueiredo and A. M. T. Silva, *J. Environ. Chem. Eng.*, 2021, **9**, 104–930.
21 C. Ferreiro, N. Villota, A. de Luis and J. I. Lombraña, *React. Chem. Eng.*, 2020, **5**, 760–778.
22 D. Wang, Z. Chen, Z. Zhou, D. Wang, J. Yu and S. Gao, *Fuel Process. Technol.*, 2019, **189**, 98–109.
23 W. Tong, Y. Xie, W. Hu, Y. Peng, W. Liu, Y. Li, Y. Zhang and Y. Wang, *RSC Adv.*, 2020, **10**, 9976–9984.
24 S. Baloyi, T. Ntho and J. Moma, *RSC Adv.*, 2018, **8**, 5197–5211.
25 D. B. Pal, A. Singh, J. M. Jha, N. Srivastava, A. Hashem, M. A. Alakeel, E. F. Abd Allah and V. K. Gupta, *Bioresour. Technol.*, 2021, **339**, 125606.
26 J. Wang, B. Hong, X. Tong and S. Qiu, *J. Air Waste Manage.*, 2016, **66**, 1268–1275.
27 S. Khoei, A. Stokes, B. Kieft, P. Kadota, S. J. Hallam and C. Eskicioglu, *Bioresour. Technol.*, 2021, **341**, 125864.
28 Y. Zhang, T. Gan, H. Hu, X. Cai, Z. Huang, X. Liang, Y. Yin, Y. Qin and Z. Feng, *J. Hazard. Mater.*, 2019, **380**, 120–892.
29 F. Shen, Y. Zhang, H. Hu, Z. Huang, Y. Yin, X. Liang, Y. Qin and J. Liang, *J. Hazard. Mater.*, 2019, **366**, 466–474.
30 S. Yang, X. Yang, X. Shao, R. Niu and L. Wang, *J. Hazard. Mater.*, 2011, **186**, 659–666.
31 M. Zhou, Q. Tan, Q. Wang, Y. Jiao, N. Oturan and M. A. Oturan, *J. Hazard. Mater.*, 2012, **215–216**, 287–293.
32 Y. Kong, Y. Zhuang and B. Shi, *J. Hazard. Mater.*, 2020, **382**, 121060–121070.
33 D. Zhao, X. Liao, X. Yan, S. G. Huling, T. Chai and H. Tao, *J. Hazard. Mater.*, 2013, **254**, 228–235.
34 G. D. Fang, D. M. Zhou and D. D. Dionysiou, *J. Hazard. Mater.*, 2013, **250**, 68–75.
35 J. Daniel Garcia Espinoza and P. Mijaylova Nacheva, *Sci. Total Environ.*, 2019, **691**, 417–429.
36 Y. Yang and F. S. Cannon, *J. Environ. Chem. Eng.*, 2021, **9**, 106391.
37 C. Liang, Y. T. Lin and W. H. Shih, *Ind. Eng. Chem. Res.*, 2009, **48**, 8373–8380.
38 Y. T. Wang, Z. Fang and X. X. Yang, *Appl. Energy*, 2017, **204**, 702–714.